Physica Scripta. Vol. T12, 70–75, 1986.

Rydberg Wave Packets and the Classical Limit

Jonathan Parker and C. R. Stroud, Jr.

The Institute of Optics, University of Rochester, Rochester, New York 14627, U.S.A.

Received March 18, 1986; accepted March 26, 1986

Abstract

A method is proposed and analyzed for producing single atom Rydberg states which are nearly as possible classical. It is shown that a picosecond laser pulse can excite a localized wave packet of Rydberg states which propagates like a particle in a classical Kepler orbit. These states are studied numerically and approximate analytic techniques are developed for analyzing their properties.

1. Introduction

Laser spectroscopy and quantum optics have made great strides in the past two decades in exploring the relationship between the classical and quantum theories of the electromagnetic field. In this volume are papers describing "nonclassical" states of the field states which are peculiarly quantum mechanical with no classical analog. A large fraction of the effort in these research areas has been devoted to the study of such states.

There is a second interface between classical and quantum theory which has become accessible for experimental investigation thanks to newly developed tools of laser spectroscopy. It is now possible to excite single atoms into states which approach the classical limit. The classical limit of a single atom has been a subject of some interest from the earliest days of quantum theory. It is the correspondence principle which leads to the proper Hamiltonian operator for an atom. Niels Bohr in 1923 [1] formulated this principle stating that classical mechanics is correct in the macroscopic regime, thus quantum theory must reduce to classical theory in the limit that the physical system described becomes macroscopic.

There are several ways in which this limit might be carried out. Many text books suggest that the macroscopic limit is approached when all quantum numbers of the system become large. If one applies this limiting process to the one-electron atom, one arrives at an eigenstate corresponding to a large orbit, but rather than a localized electron following the Kepler orbit we get a probability distribution spread throughout the orbit. Recent developments in experimental technique has made it possible to produce and study a single atom in such a limiting state. The probabilistic picture of microscopic quantum theory is hardly a proper feature of a classical system in a single realization.

Of course, the $\Delta r \Delta p$ uncertainty principle places a limit on the sharpness of the prediction even in this classical limit, but the smearing required is far less than that which we find in the energy eigenstates. Schrödinger and Lorentz studied this problem in 1926 and realized that the classical atom could be approached in a different limit [2].

Schrödinger and Lorentz studied the behavior of a wave packet made up of a coherent superposition of highly excited states. Such a wave packet can approach the ideal of a localized particle traveling in a classical orbit. Lorentz was unhappy to discover, however, that the wave packet rapidly spreads around the orbit. In a recent paper [3] we have shown that this decay of the wave packet is not necessarily irreversible, but that in certain cases the packet may later come together again in a compact form.

Schrödinger, in these studies, discovered the coherent states of the harmonic oscillator [4]. These states are minimum uncertainty wave packets whose shape remains constant as the packet moves along the classical trajectory. There have been a number of efforts over the years to develop analogous "coherent atomic states" [5–7]. These attempts have been somewhat successful, but they have suffered from the fact that there appeared to be no direct way of producing such states in the laboratory.

We have shown that if a coherent short laser pulse is used to excite an atom into a highly excited bound state, the resulting state may be quite classical. If the central frequency of the laser field and the pulse duration are chosen properly, the resulting state of the atom may be such that it oscillates almost periodically between a state well described as a minimum uncertainty wave packet, moving and radiating like a classical charged particle, and a spread-out state which is very much quantum mechanical.

It is very easy to see why short laser pulses are able to produce coherent atomic wave packets. The finite duration of a one picosecond laser pulse produces a frequency bandwidth of $20\,\mathrm{cm}^{-1}$, and for a one femtosecond pulse it produces a bandwidth of $\sim 20\,000\,\mathrm{cm}^{-1}$. If the central frequency of such a laser is tuned so as to resonantly excite an atom from the ground state to the manifold of Rydberg states, the large bandwidth will excite a coherent superposition of many Rydberg states.

In this paper we will analyze these states, both analytically and numerically, to see to what extent they are classical in nature, and will describe the experimental implications of their existence. In Section 2 we will numerically solve the semiclassical equations describing the laser excitation in several special cases and show how, under certain conditions, the laser excites these wave packets. In Section 3 we will obtain analytic solutions of the semiclassical equations and show that a simple Fermi Golden Rule analysis is appropriate. In Section 4 we will extend the theoretical analysis to a WKB treatment of the wave packet. In Section 5 we will describe the experimental implications of our calculations including quantum beat and pump-probe experiments. Finally, in section 6 we will summarize our results.

2. Short-pulse laser excitation

A simple semiclassical calculation gives an expression for this coherent superposition state. We represent the pulsed field in

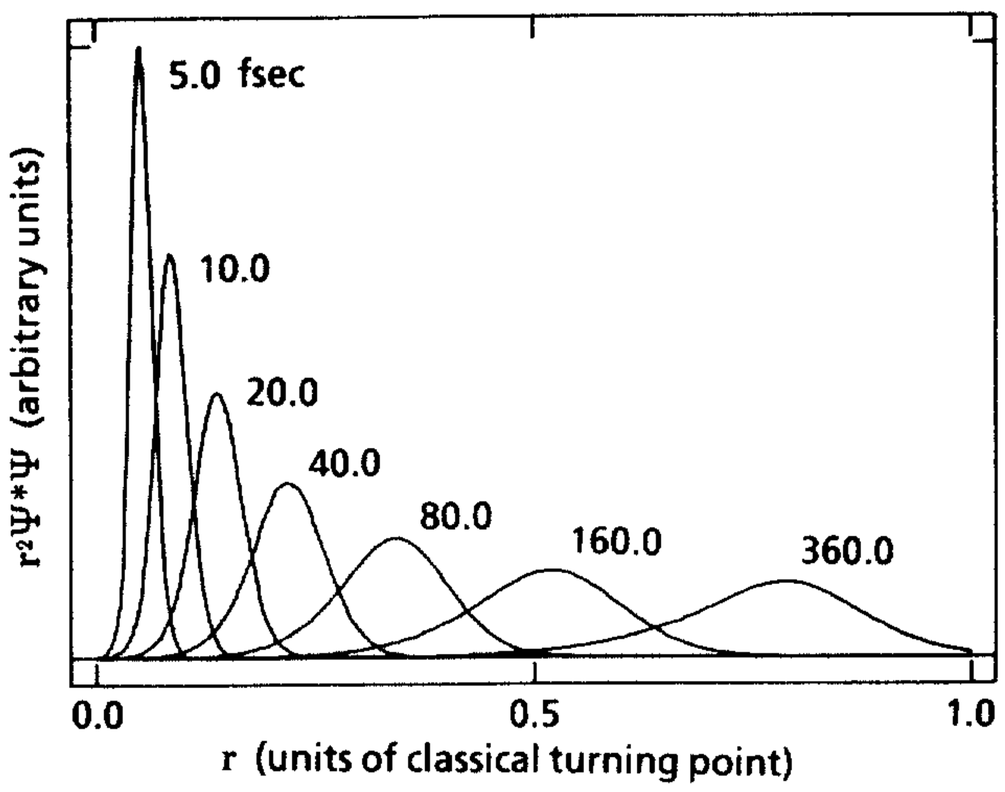

Fig. 1. Rydberg wave packets generated by pulses of various lengths. Here the packets are labeled by the pulse lengths (FWHM intensity) in femtoseconds. The laser excites Rydberg states in the vicinity of $n = 25$. The packets are as they appear when the pulse has fallen to 0.4% of its peak intensity.

the form

$$E(t) = 2E_0 f(t) \cos(\omega_0 t), \tag{1}$$

where ω_0 is the central frequency of the laser, $2E_0$ is the vector amplitude at the center of the pulse, and $f(t)$ is the pulse envelope function, which equals unity at $t = 0$, the centre of the pulse. This field, when substituted into Schrödinger's equation, leads to the amplitude equations

$$\frac{\mathrm{d}}{\mathrm{d}t} c_\varepsilon = -\mathrm{i}\Delta_\varepsilon c_\varepsilon - \frac{\mathrm{i}}{\hbar} H_{\varepsilon g} f(t) c_g \tag{2a}$$

$$\frac{\mathrm{d}}{\mathrm{d}t} c_g = -\frac{\mathrm{i}}{\hbar} \sum_\varepsilon H_{g\varepsilon} f(t) c_\varepsilon. \tag{2b}$$

In these equations quantities refering to the ground state are denoted by the subscript g, while those refering to the excited states are labeled by an index ε which may represent either a bound or continuum state. The matrix elements of the interaction Hamiltonian are written $H_{g\varepsilon} f(t)$, while the energy of state ε is written $\hbar\omega_\varepsilon$. For simplicity we have made the rotating-wave approximation, although it is quite possible to retain the counter-rotating terms in the numerical solutions of these equations. Thus detuning Δ_ε is $\omega_\varepsilon - \omega_0$, and the ground state energy has been set to zero.

We have numerically integrated these equations and substituted the solutions into the expansion for the wave function

$$\Psi(r, t) = \mathrm{e}^{-\mathrm{i}\omega_0 t} \sum_\varepsilon c_\varepsilon(t) u_\varepsilon(r). \tag{3}$$

In the numerical examples of this section, the functions $u_\varepsilon(r)$ are the radial hydrogenic wave functions. For principal quantum numbers $n = 2$ up to some upper limit n_2 they are Laguerre polynomials. At higher energies both the bound and unbound states are obtained by directly integrating Schrödinger's time-independent equation.

In Fig. 1 is shown the wave packet $r^2\Psi^*\Psi$ as it appears immediately after the end of the pulse for various pulse durations. In each case the central frequency of the laser field resonantly excites the $n = 25$ state. The amplitude of the field is adjusted so that the total pulse energy of the field is the same in each case, and is in fact the energy required to pump 10% of the population into the Rydberg states.

The bandwidth of the laser is sufficiently large so that one would expect a wavepacket to be formed in each case, and indeed it is. One can easily show that the center of the wave packet is where one would expect to find a classical particle that had been given the energy $\hbar\omega_0$ at time $t = 0$, and allowed to move freely in the Coulomb potential, starting from a point near the nucleus. The time $t = 0$ is the time at which the center of the pulse reaches the atom.

The spatial axis in Fig. 1 is labeled in units of the classical turning point of an electron with energy equal to that of state $n = 25$, and with angular momentum $\hbar$. This turning point, or apogee, is given by approximately $2n^2 a_0$ where a_0 is the Bohr radius. Thus, not only is it a well defined wave packet, but it is moving in an orbit more than 1000 a_0 in diameter.

A simple Bohr–Sommerfeld analysis shows that the classical orbital period corresponding to nth quantum state is just 2π times the reciprocal of the transition frequency between levels n and $n - 1$. One might expect to see these wave packets maintain their shape during the orbit. This happens only approximately, and only for the packets (of Fig. 1) produced by the longest laser pulses. The shorter pulses produce packets which spread and break up before reaching the apogee.

The reason for the rapid break up of the packet is easily seen. The short pulse excites a range Δn of levels about n. The classical orbital frequency is given by $\Omega_n = e^2/(a_0\hbar n^3)$, while the variation in orbital frequencies is given by $\Delta\Omega_n = 3(\Delta n/n)\Omega_n$. The condition that the wavepacket orbit the nucleus many times before breaking up is just that $\Delta\Omega_n \ll \Omega_n$ or equivalently $\Delta n \ll n$. By a very simple extension of this argument one can show that these inequalities are equivalent to $\tau_p \gg n^2\tau_0$, where τ_0 is the orbital period of the lowest Bohr orbit, 1.52×10^{-16} seconds. This inequality shows that we need a pulse duration much longer than 95 fs to produce a reasonably stable wave packet for $n = 25$.

For $n = 85$ the pulse must be longer than 1.1 ps. Figure (2a) shows the evolution of a wavepacket produced by a pulse of duration 10 ps with $n = 85$. The curves are just the packet at various times in picoseconds after the center of the pulse. The spatial coordinate is measured in terms of the classical turning point radius which is approximately 15 000 Bohr radii for $n = 85$. As the packet approaches the turning point it narrows up. The classical orbital period is 93.4 ps so the wavepacket reaches the turning point at about 47 ps, as shown in Fig. 2(b) and then begins moving backward toward the nucleus. As the packet nears the nucleus at 90 ps it is dispersed by the strong Coulomb field. As it completes its orbit and begins its return to the outer turning point it reassembles into a packet almost as compact as the original packet. The process repeats four times before the packet fails to reassemble even at the turning point.

The reason that the packet disperses at perigee (closest approach to the nucleus) and departs from the classical character it exhibits at apogee is that the superposition which makes up the wave packet does not have all quantum numbers large. The ground state is an s state so that the absorption of a single photon will result in an excited state of angular momentum $\hbar$. This low angular momentum wavepacket corresponds to a classical electron in a highly elliptical orbit.

The oscillation of the system between a nearly classical state and a quantum state is best seen by observing the evolution of the uncertainty product $\Delta r \Delta p$ as the wave packet evolves. This evolution is shown in Fig. 3. The system is

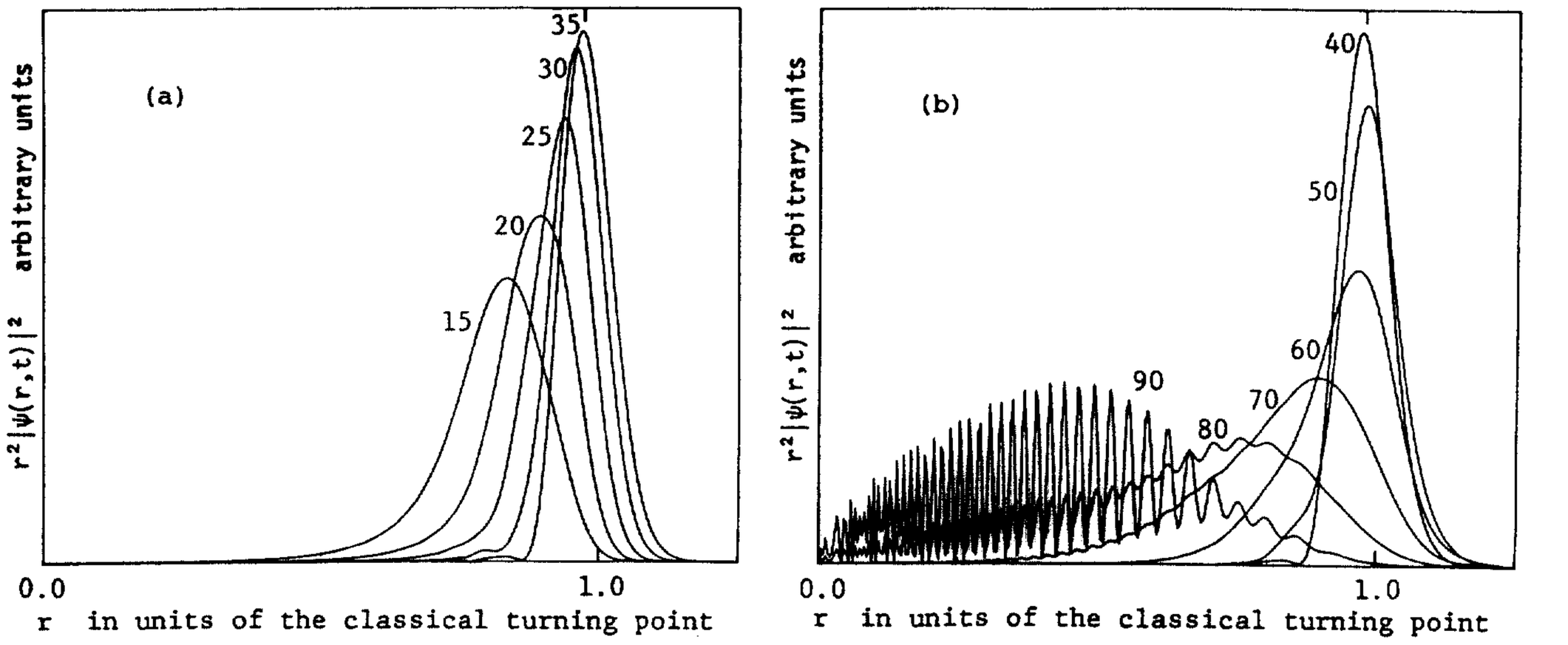

Fig. 2. Rydberg wave packet during its first orbit. Each curve is labeled by the time that has elapsed, in picoseconds, from the center of the laser pulse. A 10 ps pulse (FWHM intensity) was used to excite Rydberg states in the vicinity of $n = 85$. The wave packet during the firt half of the orbit is shown in (a); in (b) it is shown during the second half.

excited exactly as in Fig. 2. The Heisenberg uncertainty principle states that the minimum uncertainty product is $0.5\hbar$. At the first approach to the turning point the product is $0.516\hbar$, while at the second approach it is less than $3\hbar$.

Even the break up of the packet after the fourth orbit is not permanent. Because the levels are discrete, and because only a relatively small number Δn are excited, the system undergoes revivals in which the wave packet reassembles approximately. The first such revival occurs after about 28 orbits. In fact the uncertainty product is less than $13\hbar$ again after the 29th orbit.

The occurrence of only one angular momentum state in the coherent superposition making up the packet means that the spatial localization is only in the radial direction, not in the polar and azimuthal directions. The wave packet is a hollow shell oscillating in and out about the nucleus.

In this section we have seen that it is indeed possible to excite wave packets of Rydberg atomic states which travel to a certain extent along classical orbits and approach the fundamental quantum limit in the uncertainty product. Two separate conditions were found to be necessary to form these classical states. The first is that the laser pulse must have a coherent bandwidth sufficiently large to excite simultaneously a number of Rydberg states. This is equivalent to requiring that the pulse be short in comparison to the orbital period of the corresponding classical electron. The second condition sets a lower limit on pulse duration in order to produce reasonably stable wave packets. Both conditions can be combined in the form

$$n^2\tau_0 \ll \tau_p \ll n^3\tau_0, \tag{4}$$

where τ_0 is the orbital period of an electron in the first Bohr orbit.

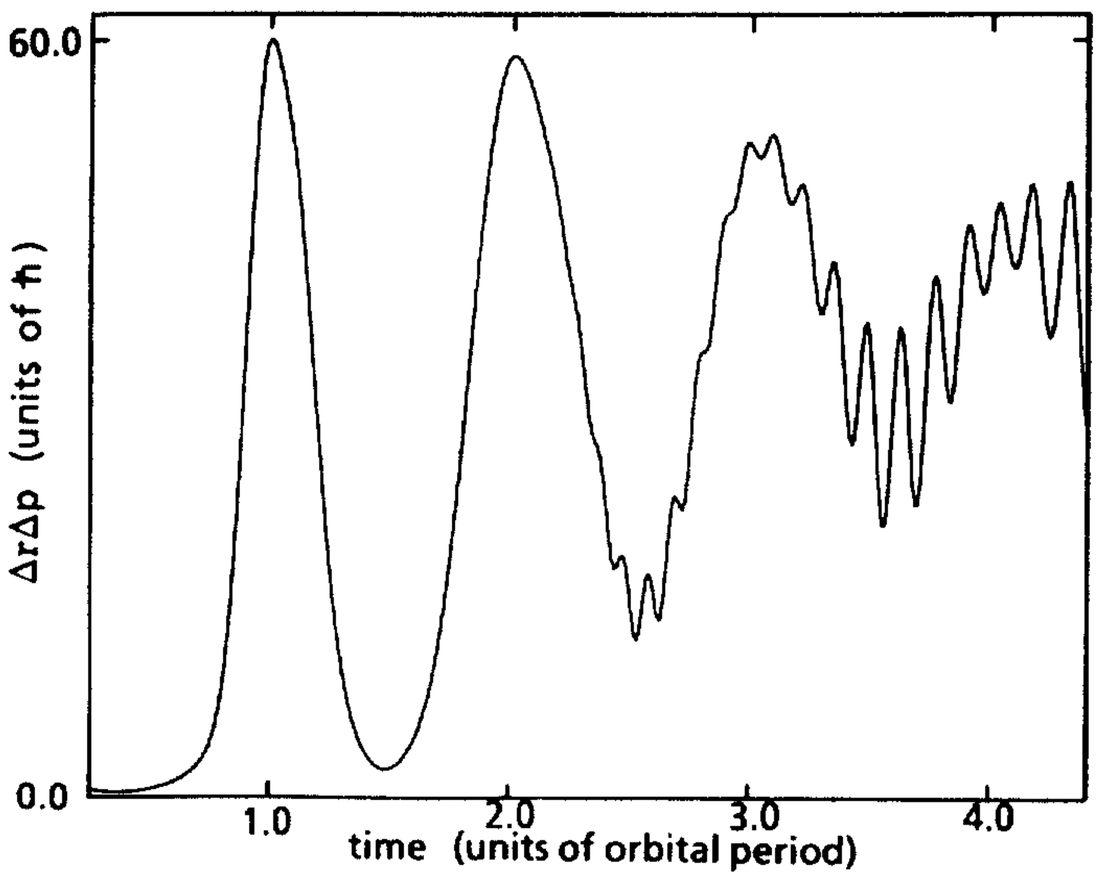

Fig. 3. The uncertainty product $\Delta r\Delta p$ of an orbiting Rydberg wave packet. The packet is as described in Fig. 2. The uncertainty product is shown over the packet's first four orbits.

3. Analysis of the equations of motion

The numerical examples and simple physical arguments of Section 2 provided a definite range of parameters for which well localized Rydberg wave packets are formed. The actual working out in detail of the shape and evolution of the wave packet is made difficult, however, by the infinite sum over Rydberg states which occurs in eq. (2) and eq. (3). In this section and the next we will work out analytic approximation techniques which greatly simplify this problem and allow us to extend our results to non-hydrogenic one-electron atoms.

We are interested in the state of the atom just at the end of the pulse, as in Fig. 1. Although the equations below generalize without difficulty to arbitrary times t, assume below that the field has died away at time t. Equation (2.2a) may be integrated formally to give,

$$c_\varepsilon(t) = -\frac{i}{\hbar} H_{\varepsilon g} F(\Delta_\varepsilon)\, e^{-i\Delta_\varepsilon t} \tag{5}$$

where $F(\Delta\varepsilon)$ is the Fourier transform of $f(t)c_g(t)$:

$$F(\Delta_\varepsilon) = \int_{-\infty}^{\infty} dt\, f(t)c_g(t)\, e^{i\Delta_\varepsilon \tau}. \tag{6}$$

We turn not to a discussion of Fermi's Golden Rule by calculating the population in the excited state at the end of the pulse:

$$\sum_\varepsilon |c_\varepsilon(t)|^2 = \hbar^{-2} \sum_\varepsilon |H_{\varepsilon g}|^2 |F(\Delta_\varepsilon)|^2. \tag{7}$$

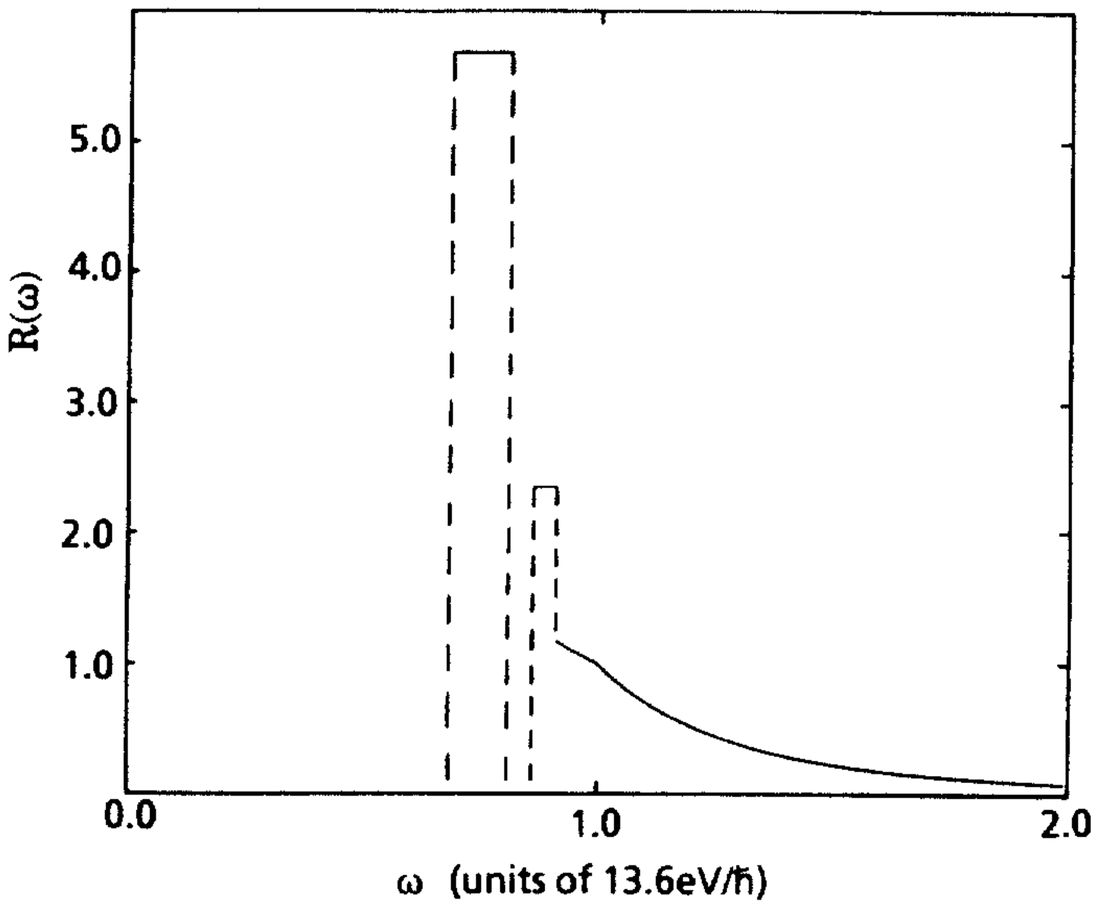

Fig. 4. Fermi Golden Rule transition rate $R(\omega)$. Here the atomic system is hydrogen and $R(\omega)$ describes a single photon transition from the ground state to an $l = 1$ excited state of energy $\hbar\omega$. The energy of the ground state ($n = 1$) has been set to zero so that $\omega = 1$ is the boundary between the bound states and the unbound states of hydrogen. In this graph $R(\omega)$ is scaled so that $R(1) = 1$.

This sum can be formally rewritten in the form of an integral

$$\sum_{\varepsilon} |c_{\varepsilon}(t)|^2 = \frac{1}{2\pi} \int d\omega\, R(\omega) |F(\omega) - \omega_0)|^2 \tag{8}$$

where $R(\omega)$ is the usual Fermi Golden Rule rate for unbound states,

$$R(\omega) = \frac{2\pi}{\hbar^2} \varrho(\omega) |H_{\omega g}|^2, \tag{9}$$

and for bound states

$$R(\omega) = \frac{2\pi}{\hbar^2} \sum_{n} \delta(\omega - \omega_n) |H_{\omega g}|^2. \tag{10}$$

Here $E_n = \hbar\omega_n$ is the energy of the hydrogenic state with principal quantum number n, and $H_{\omega g}$ equals $H_{\varepsilon g}$ with ε such that $\omega_{\varepsilon} = \omega$. The smooth shape and the finite duration of the pulse envelope $f(t)$ implies that the Fourier transform $F(\Delta)$ is smooth, changing little over the range from one bound state to the next. Thus the δ-functions in the sum (10) can be spread out into rectangles of unit area centered about E_n. These rectangles can then be spread until they all just touch. So long as the areas remain unity and the widths remain narrow compared to the width of $F(\Delta)$ the smearing of the δ-functions will not affect the value of the sum (8).

The resulting smoothed rate $R(\omega)$ is shown in Fig. 4. The curve has been made smooth except at the bound excited states of lowest energy, $n = 2$ and $n = 3$. The $n = 2$ rectangle has been drawn apart from the others to emphasize its exceptional character. If the laser is tuned to the Rydberg states, the pulse must have exceptionally large bandwidth to put population into the $n = 2$ state. Pulses short enough to excite the $n = 2$ state, pulses shorter than 5 fs (FWHM), are outside the bounds of our discussion.

Equation (8) tells us that the excited state population is proportional to the overlap of the "spectrum" $|F(\Delta)|^2$ with the rate $R(\omega)$. Let us consider (8) in the case of a Gaussian shaped pulse of duration $\tau_0 = 5$ fs (FWHM). As we explain in Section 4, the FWHM width of the spectrum $|F(\Delta)|^2$ of such a pulse is very nearly $2/\tau_0$. Its width is 1/50th of the Rydberg frequency, 13.6 eV/$\hbar$. Thus if we were to draw the curve $|F(\Delta)|^2$ on top of $R(\omega)$ in Fig. 4 we would see that $R(\omega)$ is slowly varying in comparison to the spectrum of the pulse.

These arguments lead us to the conclusion that during excitation the bound Rydberg states behave like continuum states. Of course these arguments apply only to the very short period when the pulse is applied. During this time interval the electron has not had time to move all the way out to the classical turning point of its orbit to find that is in a bound rather than an unbound state.

The smoothing and Fermi Golden Rule approximations also allow us to obtain an analytic expression for the ground state amplitude

$$c_g(t) = \exp\left[-\frac{R(\omega_0)}{2} \int_{-\infty}^{t} dt'\, f^2(t') \right]. \tag{11}$$

We conclude that the conditions which are necessary in order to produce a well-defined Rydberg wave packet are exactly those which allow us to simplify the difficult sum over an infinite number of Rydberg states into a relatively simple integral. The excitation is then well described by Fermi's Golden Rule so that the time dependence is a simple exponential depletion of the ground state without Rabi oscillations. Even though the field is fully coherent the effectively smooth continuum final state means that the excitation is described by a simple cross section.

4. WKB analysis of the wave packet

In this section we will develop approximate analytic expressions for the shape of the wave packet at the end of the laser pulse. In Section 3 we found that it is not necessary to take into account the detailed atomic level structure nor the full coherent dynamics of the excitation. Here we will see that the methods of Section 3 greatly simplify the infinite sum over the rapidly oscillating radial wave functions.

A simple calculation leads to the intuitively appealing result that the narrowest wave packet that can be produced is just the ground state probability function moved up to a Rydberg orbit. If we simply substitute eq. (5) into eq. (3) we find that the Rydberg wave function at the end of the pulse is given by

$$\Psi(r, t) = -\frac{i}{\hbar} e^{-i\omega_0 t} \sum_{\varepsilon} e^{-i\Delta_{\varepsilon} t} F(\Delta_{\varepsilon}) \langle g|H'|\varepsilon\rangle \langle \varepsilon|r\rangle \tag{12}$$

where $H' = -er \cdot E_0$. From Fig. 1 we see that the wave packet becomes narrower as the laser pulse duration becomes shorter. Consider the ultimate limit of a δ-function pulse. In that case $F(\Delta_{\varepsilon})$ becomes a constant independent of Δ_{ε}. Similarly, if we examine the wave function just after the pulse then the time-dependent factor is nearly unity. In that case we can carry out the sum over ε to find that

$$\Psi(r, t) \propto \langle g|H'|r\rangle = -er \cdot E_0 u_g(r). \tag{13}$$

The width of the wave packet is then to a good approximation just the width of the ground state.

Of course, the limiting case of a δ-function pulse is beyond the range of validity of the theory. Photoionization cannot be neglected when pulses become intense enough to excite the hydrogen atom in a few femtoseconds or less. Our analysis of

the packets of Fig. 1 will require a more sophisticated approximation scheme. There is, of course, a formal perturbation scheme which has been developed for finding classical approximations of Schrödinger's equation: the WKB method.

The WKB method gives a good approximation of the wave functions except near the turning points. The wave packets of Fig. 1 were generated by pulses that were short compared to the orbital period of the corresponding classical electron. From Fig. 1 it is clear that the packets have not reached the turning point of the state $n = 25$. More importantly it may be verified numerically that the leading edge of each packet of Fig. 1 has not reached the turning points of the states that received substantial population during the excitation. We would then expect the WKB method to accurately describe the wave packets of Fig. 1.

The WKB eigenfunction is

$$r\langle\varepsilon|r\rangle = ru_\varepsilon(r) = N_\varepsilon k_\varepsilon^{-1/2} \cos\left(\int_{r_0}^{r} dr'\, k_\varepsilon(r') - \frac{\pi}{4}\right), \quad (14a)$$

where

$$k_\varepsilon(r) = \left[\frac{2m}{\hbar^2}(\hbar\omega_\varepsilon - V(r))\right]^{1/2}, \quad (14b)$$

is $\hbar^{-1}$ times the classical momentum of the electron, and $V(r)$ is the effective potential. The normalization factor is N_ε, and r_0 is the inner turning point of the orbit (perigee).

We can make use of the WKB wave functions in eq. (12) if we first approximate the sum over ε by an integral just as we did in Section 3. We will also approximate $k_\varepsilon(r)$ by its value at $\omega_\varepsilon = \omega_0$, and we will call this new function $k_0(r)$. The time-dependent wave function is then

$$r\Psi(r, t) = Nk_0^{-1/2} \int d\Delta\, R^{1/2}(\Delta + \omega_0) F(\Delta) \times \exp\left(i\int_{r_0}^{r} dr'\, k_\varepsilon(r') - i\Delta t\right). \quad (15)$$

In deriving this expression we have dropped an overall time dependent phase factor and have kept only the part of Ψ that propagates outward toward the apogee. The normalization factor N is

$$N = \frac{1}{2\pi}\left(\frac{\hbar}{e^2 a_0}\right)^{1/2}. \quad (16)$$

In our equations we have an additional approximation available to us. The exponent in eq. (15) can be expanded about ω_0. We define Φ

$$\Phi = \frac{d}{d\omega}\int_{r_0}^{r} dr'\, k_\varepsilon(r')\Big|_{\omega=\omega_0} = \frac{\hbar}{e^2 a_0}\int_{r_0}^{r}\frac{dr'}{k_\varepsilon(r')}\Big|_{\omega=\omega_0}. \quad (17)$$

Similarly, Φ_2 is defined as the second derivative of the same integral, also evaluated at ω_0. The quantity Φ has a simple physical interpretation. It is the time required for a classical particle of energy $\hbar\omega_0$ to travel from r_0 to r. For small $\Delta\omega$, $\Phi_2\Delta\omega$ is the difference in time required for two particles of energy $\hbar\omega_0$ and $\hbar(\omega_0 + \Delta\omega)$ to travel from r_0 to r.

In the approximation in which we neglect Φ_2, Ψ is just the Fourier transform of a product of functions. Applying the convolution theorem and neglecting a phase factor we can show that

$$r\Psi(r, t) = Nk_0^{-1/2} S(t - \Phi)^*[f(t - \Phi)c_g(t - \Phi)], \quad (18a)$$

where

$$S(t) = \int_{-\infty}^{\infty} d\Delta\, R^{1/2}(\Delta + \omega_0)\, e^{-i\Delta t}. \quad (18b)$$

These approximations are consistent with those in Section 3. If we use eq. (18) to calculate the total excited state population, we find

$$\int dr\, r^2|\Psi|^2 = \frac{1}{4\pi^2}\int d\Phi\, |S(t - \Phi)^*[f(t - \Phi)c_g(t - \Phi)]|^2. \quad (19)$$

We have used $k_0^{-1}\, dr = (a_0 e^2\hbar)\, d\Phi$. Now a simple application of Parceval's theorem yields exactly our formulation of Fermi's Golden Rule, eq. (8).

In the present approximation the ultimate narrowness of Ψ, in the limit of a δ-function pulse, is given by $k_0^{-1/2} S(\Phi)/r$. However, in the case of pulse durations greater than 5 fs, $S(\Phi)$ may be replaced by a δ-function in eq. (18a). This is equivalent to replacing $R(\omega)$ with $R(\omega_0)$ in eq. (15). The result is

$$r\Psi \propto f(t - \Phi)c_g(t - \Phi)k_0^{-1/2}. \quad (20)$$

Over a wide range of conditions the position $\langle r\rangle$ of the wave packet predicted numerically as in Fig. 1 is in agreement with that predicted by eq. (20). Over the range of pulse durations from 5 fs to 200 fs the agreement is to within 1%. Even at 1 fs there is agreement to within 2%.

In the weak field limit, $c_g \approx 1$, eq. (20) predicts that the position of the packet at time t is the position a classical particle, originally at r_0, which was abruptly given the energy $\hbar\omega_0 = 0$. In stronger fields the effect of $c_g(t)$ is to shift the peak of the packet to regions of greater r, but $c_g(t)$ cannot shift the leading edge of the wave packet. The classical character of WKB wave packets has been discussed in greater detail by Brown [8].

The wave packets at the end of the pulse may have a $\Delta r\Delta p$ uncertainty product which approaches the Heinsenberg minimum. The generality of this result may be seen by some simple arguments. The exciting laser pulse envelope $f^2(t)$ and its Fourier transform satisfy the relation $\Delta\omega\Delta t \approx 1$, i.e. the product of the standard deviation widths of the function in ω-space and t-space is about unity. If we multiply each side of this relation by $\hbar$, we get $\Delta E\Delta t \approx \hbar$, which is often called the time-energy uncertainty relation.

The excited state probability $|c_\varepsilon|^2$ is seen from eq. (8) to be proportional to the absolute square of the Fourier transform of $f(t)c_g(t)$. The proportionality factor $R(\omega)$, is only very slowly dependent on ω. Thus the spread in energy is the same as $\hbar$ times the spread in the square modulus of the Fourier transform of $f(t)c_g(t)$.

If we define Δt of the packet to travel a distance equal to its width Δr, then it follows from eq. (20) that the Δt of the packet $r^2\Psi^*\Psi$ is very nearly that of the "pulse", $f^2(t)c_g^2(t)$. The result is that the $\Delta E\Delta t$ product of the WKB wave packet is the same as that of the pulse that excited it. For a Gaussian pulse, the product $\Delta E\Delta t$ is equal to $\hbar/2$. Even though $f(t)c_g(t)$ is not Gaussian, and $R(\omega)$ is not constant, it is found numerically that the wave packets of Fig. 1 have a $\Delta E\Delta t$ product within a few percent of $\hbar/2$.

Our definition of Δt is a natural one, and it is the one

generally used to establish the equality $\Delta r \Delta p = \Delta E \Delta t$ for a freely propagating wave packet [9]. Despite the fact that the packets of Fig. 1 are in the Coulomb potential, a numerical calculation of $\Delta r \Delta p$ at the end of the pulse verifies that these packets are very nearly minimum uncertainty in $\Delta r \Delta p$ as well as $\Delta E \Delta t$. In fact $\Delta r \Delta p$ is less than $0.6\hbar$ for each of the packets shown in Fig. 1. This is true only for a brief interval near the end of the pulse, as in the case shown in Fig. 3.

Spreading of the wave packet may be investigated in the usual way. The pulse $f(t)c_g(t)$ is approximated as a Gaussian, the $\Phi_2 \Delta^2$ term is kept in eq. (15) and then the equation is integrated directly. The result is the same that is found for the case of a free particle wave packet [10]. The packet spreads like a packet of classical particles with the same distribution in energy as the quantum mechanical state.

Moreover, we may justify our previous neglect of Φ_2 for times during the pulse and shortly thereafter. One finds that Φ_2 gives a significant contribution to the width of Ψ for early times only when the pulse duration approaches a single optical period.

5. Experimental implications

The laser parameters required to produce the wave packets we have discussed are well within current technology if the initial atomic state is not the ground state but rather some excited state a few eV above the ground state. The problem is further simplified if the experiment is carried out not in hydrogen but in one of the alkalis. As we saw in Section 3, the excitation process does not depend on the detailed level structure, but only on a smoothed transition function $R(\omega)$ as illustrated in Fig. 4. Such functions look very much the same for alkalis as for hydrogen. Even after excitation most of the same analysis applies. To include the effects of core polarization in our WKB analysis, we must simply replace the effective potential of eq. (14b) by the appropriate potential for the alkali atom.

In Ref. [3] we have shown that the wave packet motion is directly reflected in the time-dependent fluorescent intensity of the atom. The quantum analog of the Larmor radiation formula predicts that the atom will send out a pulse of radiation every time that the packet is accelerated when it rounds the inner turning point. When the packet moves out to the outer turning point the acceleration is small and there is little radiation. As the packet spreads the modulation in the fluorescent intensity goes away. We will not go into detail on these predictions here, but will refer the reader to Ref. [3].

This modulation in the fluorescent intensity is also interpretable as a many level quantum beat. It provides a very direct probe of the evolution of the wave packet. Unfortunately, the fluorescent life time of the Rydberg states is extremely long – typically hundreds of microseconds to milliseconds or longer. The fluorescent signal is correspondingly weak.

A more realistic method of experimentally studying the wave packet evolution is to send in a probe laser pulse some time after the initial laser pulse. The probe will strongly interact with the wave packet when the packet is near the nucleus, and will not interact when the packet is near the outer turning point. By varying the delay between the exciting and probe pulses the evolution can be mapped out.

6. Summary and conclusions

We have seen that short coherent laser pulses can excite a hydrogen or alkali atom into a state which is a well defined wave packet moving in a classical Kepler orbit. The regime in which the oscillating wavepackets can be formed is delimited by the inequality

$$n^2 \tau_0 \ll \tau_p \ll n^3 \tau_0.$$

A number of numerical examples were shown, and in addition analytic approximation techniques were given. The analysis showed that neither the detailed level structure nor the coherent dynamics are important in the excitation process, but that a simple Fermi Golden Rule analysis applies. The analysis also showed that much of the dynamics of the packet can be understood by considering the classical motion of an ensemble of non-interacting particles with an energy distribution corresponding the spectrum of the laser pulse. It was pointed out that the evolution of the wave packet can in principle be observed in the fluorescent intensity or in a pump-probe experiment.

Acknowledgements

We would like to thank Stig Stenholm and Nordita for organizing and supporting the conference at which this work was first presented. We would also like to thank G. Alber, H. Risch, and P. Zoller for sharing with us a preprint of their work along similar lines to that presented here. We would like to acknowledge the support of the Joint Services Optics Program.

References

1. Bohr, N., Z. Physik, **13**, 117 (1923).
2. Letters on Wave Mechanics (Edited by K. Przibram), pp. 55–75, Philosophical Library (1967).
3. Parker, J. and Stroud, C. R. Jr., Phys Rev. Lett. **56**, 716 (1986).
4. Schrödinger, E., Natürwiss. **28**, 664 (1926).
5. Perelomov, M., Commun. Math. Phys. **26**, 222 (1972).
6. Nieto, M. M. and Simmons, L. M. Jr., Phys. Rev. **D20**, 1321 (1979); Nieto, M. M., Phys. Rev. **D22**, 391 (1980).
7. Gerry, C., Phys. Rev. **A33**, 6 (1986).
8. Brown, L. S., Am. J. Phys. **40**, 371 (1972).
9. Park, D., Introduction to Quantum Theory, p. 49, McGraw-Hill, New York (1974).
10. Cohen-Tannoudji, C., Diu, B. and Laloë, F., Quantum Mechanics, p. 65, Wiley-Interscience (1977).